Silicic acid dynamics in the glacial sub-Antarctic: Implications for the silicic acid leakage hypothesis

Charlotte P. Beucher,[1] Mark A. Brzezinski,[2] and Xavier Crosta[3]

Received 26 April 2006; revised 11 April 2007; accepted 31 May 2007; published 29 August 2007.

[1] The silicic acid leakage hypothesis (SALH) purports that changes in silicon and nitrogen depletion ratios in the glacial Antarctic created a large pool of unused silicic acid that was transported to lower latitudes in subantarctic mode water (SAMW) where it enhanced diatom productivity lowering atmospheric pCO_2. However, increased opal accumulation beneath the sub-Antarctic during glacial times implies significant consumption of silicic acid in subantarctic surface waters that may have significantly diminished or eliminated Si leakage. To test how nutrient dynamics in the sub-Antarctic affected the $Si(OH)_4$ content of SAMW during the last glacial period, we produced $\delta^{30}Si$ opal records for cores from the subantarctic and subtropical zones of the Indian Ocean spanning the last 50,000 years. Comparison with diatom-bound $\delta^{15}N$ records shows that subantarctic surface waters were enriched in Si relative to N during the last glaciation consistent with the SALH. The record from the subtropics does not show this enrichment in Si during the last glacial period suggesting that subantarctic surface waters were mainly incorporated into SAMW rather than being transported across the Subtropical Front. Isotope mass balance calculations were used to test for Si leakage from the sub-Antarctic. The results show that silicic acid concentration in SAMW would more than double during the last glaciation if upwelling and northward Ekman drift in the Antarctic were similar to the present-day circulation. Calculations that assume increased stratification in the glacial Antarctic eliminate Si leakage, but they do not produce the known increase in opal burial in the glacial sub-Antarctic. Reconciling the isotope data and opal burial records with a highly stratified Antarctic requires the addition of a large local source of silicic acid in the glacial sub-Antarctic that is inconsistent with present-day circulation and nutrient distributions. Including such a source in our calculations results in significant opal burial in the sub-Antarctic, but it does not enhance Si leakage over that occurring in the Holocene. Resolving past changes in the circulation of the Southern Ocean is clearly vital to future tests of the SALH.

Citation: Beucher, C. P., M. A. Brzezinski, and X. Crosta (2007), Silicic acid dynamics in the glacial sub-Antarctic: Implications for the silicic acid leakage hypothesis, *Global Biogeochem. Cycles*, *21*, GB3015, doi:10.1029/2006GB002746.

1. Introduction

[2] The silicic acid leakage hypothesis (SALH) [*Nozaki and Yamamoto*, 2001; *Brzezinski et al.*, 2002; *Matsumoto et al.*, 2002] suggests that declines in diatom $Si(OH)_4$:NO_3^- uptake ratios during glacial times created a pool of unused silicic acid in Southern Ocean surface waters that was transported to low latitudes through the formation of subantarctic mode water (SAMW). The increased silicic acid supply to low-latitude surface waters would induce a floristic shift away from cocolithophores to diatoms, lowering atmospheric pCO_2 by increasing ocean alkalinity through reduced calcite export and a higher organic carbon/$CaCO_3$ rain ratio [*Nozaki and Yamamoto*, 2001; *Brzezinski et al.*, 2002; *Matsumoto et al.*, 2002]. The decline in diatom Si:N uptake ratios required to create the pool of unused $Si(OH)_4$ in the Southern Ocean is hypothesized to have occurred as the result of a physiological response of diatoms to the increased iron flux to the region during glacial times [*Andersen et al.*, 1998; *Mahowald et al.*, 1999].

[3] Iron stress causes diatoms to reduce their carbon and nitrogen content while simultaneously increasing the amount of silica in their cell walls [*Hutchins and Bruland*, 1998; *Takeda*, 1998; *Franck et al.*, 2003]. This effect results in the greater consumption of silicic acid compared to nitrate in the present-day low-iron waters of the Southern Ocean. The $Si(OH)_4$:NO_3^- depletion ratio in the present Southern Ocean is ~4:1 [*Pondaven et al.*, 2000, and references therein; *Brzezinski et al.*, 2001] as opposed to

[1]Marine Science Institute, University of California, Santa Barbara, California, USA.
[2]Department of Ecology Evolution and Marine Biology and Marine Science Institute, University of California, Santa Barbara, California, USA.
[3]UMR-CNRS 5805 EPOC, Université Bordeaux I, Talence, France.

0886-6236/07/2006GB002746

the ratio of 1:1 observed for diatoms under conditions of adequate light and nutrients (including iron) [*Brzezinski*, 1985]. Thus the modern Southern Ocean is characterized by $Si(OH)_4$-poor and NO_3^--rich waters. This situation may have been reversed during glacial times when higher rates of dust deposition increased the supply of iron to the Southern Ocean lowering $Si(OH)_4$:NO_3^- depletion ratios [*Brzezinski et al.*, 2002]. Support for this physiological response comes from both bottle incubation experiments and from in situ iron enrichment studies in the modern Southern Ocean where additions of Fe to Antarctic surface waters favors the depletion of NO_3^- over $Si(OH)_4$ [e.g., *Boyd et al.*, 2001; *Coale et al.*, 2004; *Franck et al.*, 2003, 2005]. The evidence for a change in nutrient depletion ratios during glacial times comes from silicon and nitrogen isotopic records from Antarctic sediment cores. These two proxies are inversely correlated with minima in δ^{30}Si and maxima in δ^{15}N during glacial periods implying diminished $Si(OH)_4$ use and enhanced NO_3^- depletion [*Brzezinski et al.*, 2002]. Presumably the resulting pool of unused $Si(OH)_4$ would have been carried northward into the sub-Antarctic by Ekman drift and become incorporated into SAMW. It is currently unclear whether phytoplankton dynamics in the glacial sub-Antarctic would have consumed the excess Si delivered from the Antarctic eliminating Si leakage or whether increased dust inputs to the glacial sub-Antarctic would have lowered local $Si(OH)_4$:NO_3^- depletion ratios sufficiently to maintain the excess of Si in surface waters facilitating Si leakage.

[4] Nutrient dynamics in the glacial sub-Antarctic are highly debated. Some studies support greater nutrient depletion during ice ages [*Rosenthal et al.*, 1997, 2000; *Robinson et al.*, 2005] but others do not [*Kumar et al.*, 1995; *François et al.*, 1997; *Elderfield and Rickaby*, 2000]. The northward migration of the Southern Ocean sedimentary opal belt during glacial times [*Charles et al.*, 1991; *Mortlock et al.*, 1991] is strong evidence for substantial increases in both the supply of $Si(OH)_4$ to surface waters in the glacial sub-Antarctic and for its consumption by diatoms. The fraction of this supply that was derived from the Antarctic zone through transport by Ekman drift depends on the position of the westerly winds that drive upwelling in the Antarctic and upon the degree of stratification of Antarctic surface waters [*Sigman and Boyle*, 2000; *Anderson et al.*, 2002]. Scenarios that combine increased stratification in the Antarctic with a northerly shift in the position of the westerly winds during glacial periods [e.g., *Toggweiler et al.*, 2006] result in a reduction in the supply of $Si(OH)_4$ to the sub-Antarctic during cold periods for two reasons. First, the supply of $Si(OH)_4$ from the Antarctic would have been severely curtailed owing to less upwelling of deep waters to the south of the Antarctic Polar Front. In addition, upwelling in the sub-Antarctic would have ventilated intermediate waters with lower nutrient content than the deep waters upwelled in the Antarctic [*Anderson et al.*, 2002]. A diminished supply of $Si(OH)_4$ to the glacial sub-Antarctic is difficult to reconcile with observations of increased in opal accumulation beneath the sub-Antarctic during glacial periods [e.g., *Chase et al.*, 2003; *Dézileau et al.*, 2003]. Alternatively, the westerly winds may have remained in their modern-day position or have shifted southward maintaining Ekman flow close to its modern state [*Keeling and Visbeck*, 2001]. Under these conditions increased Fe inputs from dust and increased seasonal ice cover would act together to lessen $Si(OH)_4$ depletion in the Antarctic [*Kohfeld et al.*, 2005] resulting in an enhanced delivery of $Si(OH)_4$ to the sub-Antarctic by Ekman flow. The effect of this enhanced supply on the silicic acid concentration in SAMW depends critically on the level of silicic acid consumption in the sub-Antarctic.

[5] Changes in opal accumulation rates beneath the Antarctic Circumpolar Current (ACC) during glacial times provide some insight into how much of the $Si(OH)_4$ supplied to the sub-Antarctic was incorporated into SAMW versus being exported to depth as diatom opal. If the amount of $Si(OH)_4$ upwelled in the glacial Southern Ocean was the same as in the present day, then silicic acid leakage was only possible if the amount of opal buried in the Southern Ocean (Antarctic + sub-Antarctic) was less during glacial times compared to the Holocene. The available opal accumulation rate data suggest little change in the total amount of opal accumulation beneath the Atlantic sector of the Southern Ocean between glacial and interglacial periods [*François et al.*, 1997; *Frank et al.*, 2000]. Thus, if the $Si(OH)_4$ supply to Southern Ocean surface waters was unchanged from the present during the Last Glacial Maximum (LGM), then the amount of $Si(OH)_4$ transported to low latitudes in SAMW from the glacial Atlantic would be the same as during the Holocene. In contrast, lower rates of total (Antarctic + sub-Antarctic) opal accumulation have been documented in both the Pacific and the Indian sectors of the Southern Ocean during the LGM [*Chase et al.*, 2003; *Dézileau et al.*, 2003], which is consistent with an enhanced leakage of silicic acid during glacial periods in these sectors.

[6] The observed decline in opal accumulation in the Pacific and the Indian sectors during glacial periods could also have resulted from a reduction in the supply of $Si(OH)_4$ to Southern Ocean surface waters due to increased stratification in the Antarctic [*François et al.*, 1997; *Sigman and Boyle*, 2000]. However, a strong reduction in the supply of $Si(OH)_4$ to the sub-Antarctic from the Antarctic would work against the observed increase in opal accumulation beneath the sub-Antarctic during cold periods [*François et al.*, 1997; *Chase et al.*, 2003]. Presumably higher rates of opal accumulation in the sub-Antarctic could have been supported by the more intense upwelling in this zone during glacial periods [*Sigman and Boyle*, 2000], but as discussed above the position of the westerly winds that would have driven this flow are still debated. However, it is clear that the magnitude of the nutrient supply to subantarctic surface waters is a key factor influencing the magnitude of Si leakage from the sub-Antarctic.

[7] The study of past nutrient dynamics in the surface ocean has recently benefited from a new proxy for silicic acid use. In the late 1990s, *De La Rocha et al.* [1996, 1997] discovered that diatoms discriminate against heavy isotopes of silicon while building their frustules suggesting that the silicon isotopic composition of diatom opal may be used to reconstruct the cycling of silicon within the surface ocean [*De La Rocha et al.*, 1997]. Silicon has three major stable

isotopes: ^{28}Si, ^{29}Si, and ^{30}Si with abundances of 92.22%, 4.68%, and 3.08%, respectively [*Rosman and Taylor*, 1998]. The relative proportion of these isotopes is expressed using delta notation, $\delta^{30}Si$, where the ratio of $^{30}Si/^{28}Si$ in the sample is expressed relative to that in the NBS28 standard: $\delta^{30}Si = [(R_{sam}/R_{std}) - 1] \times 1000$ (‰), where R_{sam} and R_{std} are the ratio of ^{30}Si to ^{28}Si in the sample and the NBS28 standard, respectively [*De La Rocha et al.*, 1996]. The extent of isotopic fractionation between biogenic silica and silicic acid is defined as the fractionation factor, $\varepsilon = [(R_{bSiO2}/R_{Si(OH)4}) - 1] \times 1000$ (‰) where again $R = ^{30}Si/^{28}Si$ and the subscripts $bSiO_2$ and $Si(OH)_4$ denote biogenic silica from diatoms and silicic acid, respectively. Epsilon has a value of −1.1‰ and appears constant with species and temperature (temperature range tested 12°C to 22°C) [*De La Rocha et al.*, 1997].

[8] Interpretation of variations in $\delta^{30}Si$ in diatoms recovered from sediment cores is typically done in the context of either an open or closed system isotope model [*Varela et al.*, 2004]. In the closed system model it is assumed that the silicic acid taken up by diatoms is supplied from a finite pool of $Si(OH)_4$. In this case changes in the isotopic composition of silicic acid and of diatom silica as the silicic acid is consumed follow Rayleigh kinetics [see *De La Rocha et al.*, 1997]. As the initial pool of $Si(OH)_4$ is taken up by the diatoms the preferential incorporation of the lighter isotopes into diatom frustules causes the $^{30}Si/^{28}Si$ of the remaining $Si(OH)_4$ to increase. Subsequent diatom growth results in frustules that have increasingly positive $^{30}Si/^{28}Si$ ratios. Thus greater depletion of the available silicic acid in a closed system results in more positive values of $\delta^{30}Si$ in diatom opal. In the open system model silicic acid is assumed to be supplied continuously rather than as a finite pool. With this model diatom $\delta^{30}Si$ also becomes more positive with greater levels of silicic acid depletion, but the quantitative relationship between changes in the $\delta^{30}Si$ of opal and that of the dissolved $Si(OH)_4$ pool differ from the Rayleigh model [*Varela et al.*, 2004]. Thus, with either model, the silicon isotopic composition of diatom opal recovered from sediment cores is proportional to the level of silicic acid depletion in the overlying surface waters, but quantitative reconstruction of Si dynamics requires knowledge of whether the system studied conforms to the open or closed system model [*Varela et al.*, 2004].

[9] The SALH was developed in part by comparing $\delta^{30}Si$ records with those of the $\delta^{15}N$ of sedimentary organic matter [*Brzezinski et al.*, 2002]. The $\delta^{15}N$ of sedimentary organic matter is used as a proxy for relative nitrate use in surface waters. Its application depends upon the biological fractionation of nitrate-nitrogen and relies on the same isotope models and assumptions presented above for $\delta^{30}Si$. Phytoplankton preferentially takes up NO_3^- bearing the lighter N isotope, ^{14}N. As the NO_3^- supply is progressively consumed, the $\delta^{15}N$ of the NO_3^- increases ($^{15}N/^{14}N$ increases), leading to an increase in the $\delta^{15}N$ of the organic matter produced from the NO_3^-. This simple conceptual model is complicated by several factors other than nitrate use that alter $\delta^{15}N$ including significant changes in the $\delta^{15}N$ of bulk sedimentary organic matter during sediment diagenesis [*Altabet and Francois*, 1994], by apparent regional variations in the fractionation factor, ε [*DiFiore et al.*, 2006, and references therein] and by disagreement among $\delta^{15}N$ values produced by different analytical methods [*Robinson et al.*, 2004]. The diagenetic effect can be avoided by measuring the $\delta^{15}N$ of the nitrogen bound within diatom frustules because it is protected from degradation and alteration during burial [*Robinson et al.*, 2004, and references therein]. Resolving the analytical differences and understanding regional variation in ε remain challenges for the future.

[10] In the present study we use sedimentary $\delta^{30}Si$ opal records over the last 50,000 years from cores recovered from the subantarctic and subtropical zones of the Indian Ocean to help test the SALH. Comparison of our $\delta^{30}Si$ opal records to previously published diatom-bound $\delta^{15}N$ records [*Crosta et al.*, 2005] from the same cores indicates that less silicic acid and more nitrate were consumed in the glacial sub-Antarctic compared to the Holocene as required by the SALH. In the subtropics the enrichment of surface waters in silicic acid did not occur indicating that subantarctic surface waters were largely incorporated into SAMW during the last glacial period rather than being transported across the Subtropical Front. Using isotope mass balance calculations we show that the level of Si leakage implied by the Si isotope records is strongly dependent on the assumed circulation of the Southern Ocean during the last glacial period. A more stratified Antarctic Ocean eliminates Si leakage whereas circulation comparable to that of the modern ocean enhances Si leakage during the last glacial by over twofold compared to the Holocene.

2. Materials and Methods

[11] Down-core profiles of diatom silicon isotope composition were obtained from subantarctic piston core MD88-769 (46°04′S–90°06′E, water depth 3400 m) and subtropical piston core MD97-2101 (43°30′S–79°50′E, water depth 3200 m). MD88-769 was retrieved during the APSARA cruise at the location of the modern Subantarctic Front (SAF) (Figure 1). MD97-2101 was retrieved during the Image 3 IPHIS cruise in the vicinity of the modern Southern Subtropical Front (SSTF) (Figure 1). The age model for MD88-769 is based on 9 AMS ^{14}C dates from monospecific samples of *G. bulloides* and the age model for MD97-2101 is based on 7 AMS ^{14}C dates from monospecific samples of *N. pachyderma*, the errors on the ages are reported by *Crosta et al.* [2005]. Ages between ^{14}C dates were calculated by linear interpolation.

[12] The separation and cleaning of the diatoms from the cores followed *Singer and Shemesh* [1995] and *Crosta and Shemesh* [2002]. Cleaned diatoms were subjected to several (2 to 6) additional density gradient separations using a sodium polytungstate solution (ρ = 2.3 g cm^{-3}) to ensure the removal of aluminosilicates and metal oxides. The elimination of mineral phases was confirmed in selected samples by polarized microscopy. None of these treatments affects the silicon isotope composition of the opal [*De la Rocha et al.*, 1998].

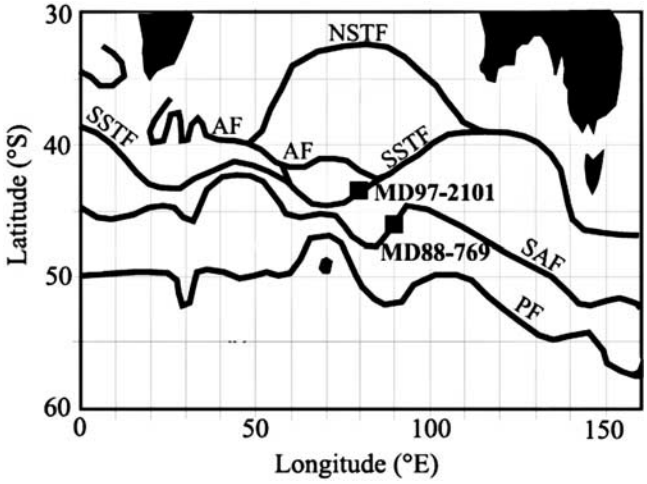

Figure 1. Location of the two cores within the different zones and fronts of the Indian Southern Ocean after *Belkin and Gordon* [1996]. NSTF and SSTF, North and South Subtropical Front; SAF, Subantarctic Front; PF, Polar Front; and AF, Agulhas Front (retroflection of the Agulhas current).

[13] A new method was used to measure silicon isotopic composition [*Brzezinski et al.*, 2006]. Cleaned diatoms were prepared for analysis by dissolution in 2.9 M HF followed by precipitation as triethylamine silicomolybdate and combustion of the precipitate to produce SiO_2 [*De La Rocha et al.*, 1996]. The SiO_2 was converted to Cs_2SiF_6 by dissolution in HF and addition of CsCl. The Cs_2SiF_6 was recovered and decomposed with H_2SO_4 to generate SiF_4 gas in a modified Finnigan Kiel III "carbonate device" in line with a Finnigan MAT 252 gas source isotope ratio mass spectrometer. Silicon isotope ratio variations are reported as delta values relative to the standard NBS28. Reproducibility for δ^{30}Si is better than ±0.07‰.

[14] Diatom-bound δ^{15}N data for each core are from *Crosta et al.* [2005]. Opal content for MD88-769 is from *Dézileau et al.* [2000] and opal rain rates are from *Dézileau et al.* [2003]. No data on opal content or opal rain rates are available for core MD97-2101. Otherwise specified δ^{30}Si and δ^{15}N notations refer to opal and diatom-bound isotopic composition.

3. Results and Discussion

3.1. The δ^{30}Si Compared to Previously Published δ^{15}N and Opal Rain Rate Records

3.1.1. Sub-Antarctic

[15] The record from subantarctic core MD88-769 shows large-amplitude variations in δ^{30}Si over the past 30,000 years; δ^{30}Si values range from +1.03 to +2.00‰ with generally lower values during the last glaciation (Figure 2). The average value of δ^{30}Si during the LGM (19–23 kyr) is lower than the average value for the Holocene (+1.4‰ LGM versus +1.9‰ Holocene) (Table 1), implying less relative $Si(OH)_4$ depletion during the LGM. Trends in δ^{30}Si generally parallel changes in sea surface temperature (Figure 2). δ^{30}Si and δ^{15}N are inversely correlated throughout the record (Figure 2) with lower δ^{30}Si, but higher δ^{15}N, during the glacial period similar to past observations from the Antarctic [*Brzezinski et al.*, 2002]. Interestingly, the Si and N isotope records appear to diverge most strongly just prior to deglaciation, but this may be an artifact given the variability in each record. Opal content decreases from 45% during MIS 3 (24–60 kyr) to 10% during the Holocene. Opal rain rates, corrected for sediment focusing (^{230}Th correction) and dissolution [*Dézileau et al.*, 2003], decline from 0.3 to 0.1 g cm^{-2} kyr^{-1} over this same time interval (Figure 2). Opal rain rates during the LGM are nearly three times higher than during the Holocene (Figure 2) suggesting enhanced diatom productivity during the ice age.

3.1.2. Subtropics

[16] The time course of δ^{30}Si in the subtropical core MD97-2101 roughly parallels the evolution of SST with values between +1.05 and +1.58‰ (Figure 3). The δ^{30}Si is minimum during the LGM (19–23 kyr) and increases gradually to the Holocene. Holocene values average +1.4‰

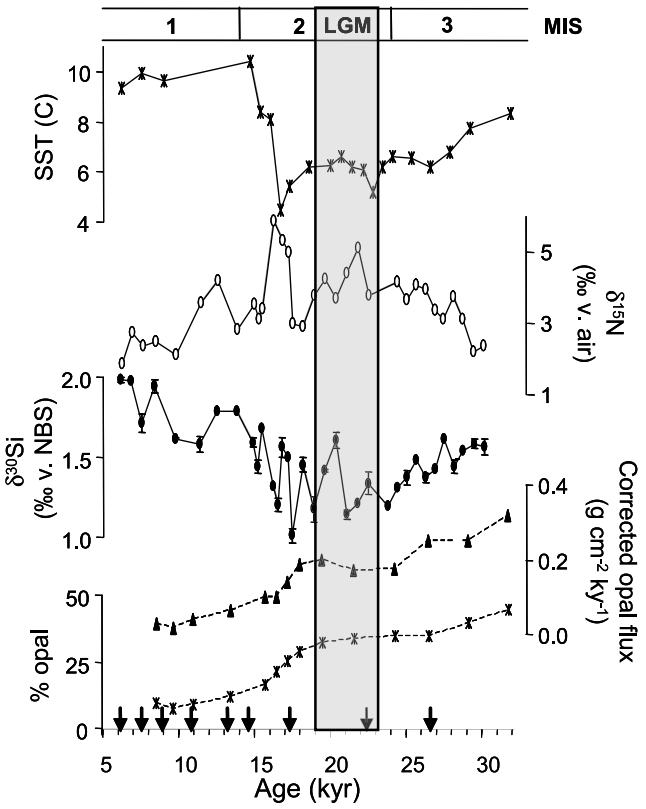

Figure 2. Down-core profiles of estimated sea surface temperatures (SST), diatom-bound nitrogen isotopes δ^{15}N [*Crosta et al.*, 2005], diatom silicon isotopes δ^{30}Si, Th-normalized and dissolution-corrected opal rain rate [*Dézileau et al.*, 2003], and opal content (% opal) [*Dézileau et al.*, 2000] versus age from subantarctic core MD88-769. Error bars on δ^{30}Si represent 1 standard deviation. Black arrows represent the location of the ^{14}C ages. LGM = 19 to 23 ka according to EPILOG (Environmental Processes of the Ice Age: Land, Oceans, Glaciers).

Table 1. Average δ^{30}Si of Opal in the Different Zones of the Southern Indian Ocean for the Holocene and the Last Glacial Maximum

	δ^{30}Si, ‰	
	Holocene	LGM
Antarctic[a]	1.4	0.9
Sub-Antarctic[b]	1.9	1.4
Subtropical[b]	1.4	1.1

[a]*De La Rocha et al.* [1998].
[b]This study.

(Table 1), similar to the δ^{30}Si values observed during MIS 3. Unlike the pattern in the sub-Antarctic, δ^{15}N and δ^{30}Si records are positively correlated in the subtropical core with both minimums coinciding with the LGM (Figure 3). Opal content and opal fluxes are not available for MD97-2101. However, opal content and opal rain rates corrected from sediment redistribution (^{230}Th correction) and dissolution have been measured in the nearby core MD94-102 (43.50°S–79.80°E, water depth 3205 m [*Dézileau et al.*, 2000, 2003]). The MD94-102 core shows low opal content (<10%) and low corrected opal rain rate (0.08 to 0.18 g cm^{-2} kyr^{-1}) during the Holocene, MIS 2 and MIS 3. Opal rain rates are higher during the LGM (0.16 g cm^{-2} kyr^{-1}) compared to 0.09 g cm^{-2} kyr^{-1} for the Holocene.

3.2. Links to Dust and Fe

3.2.1. Sub-Antarctic

[17] It is generally accepted that the supply of iron to the Southern Ocean from atmospheric dust inputs was higher during glacial periods. Elevated dust levels during glacial periods are seen in records from both Southern Ocean sediments and from Antarctic ice cores (reviewed by *Kohfeld and Harrison* [2001]). To investigate whether increased dust inputs altered patterns of silicic acid depletion in MD88-769, we compare our δ^{30}Si records with the dust record from the Vostok and EPICA Dome C ice cores (Figure 4). The increase in dust during the first half of MIS 2 (20−24 kyr) in the ice core records is accompanied by a decline in δ^{30}Si of approximately 0.6‰ in the sub-Antarctic. The low values of δ^{30}Si during MIS 2 coincide with the higher dust inputs during this period.

[18] A closer examination of the relationship between dust supply and diatom δ^{30}Si reveals that the diatoms may have responded to variations in dust throughout MIS 2. Acknowledging the limitations of the age models in our records, we found that each of the minima in the δ^{30}Si record from the sub-Antarctic during the glacial period in MD88-769 coincides in time with peaks of dust deposition at Vostok (Figure 4). Dust/iron deposition and silicon isotope composition are inversely correlated with $R^2 = 0.61$ ($n = 26$, $p < 0.05$; Figure 5a). Further evidence for a close coupling between dust and δ^{30}Si in the sub-Antarctic is revealed by comparing the first derivative of the Vostok dust

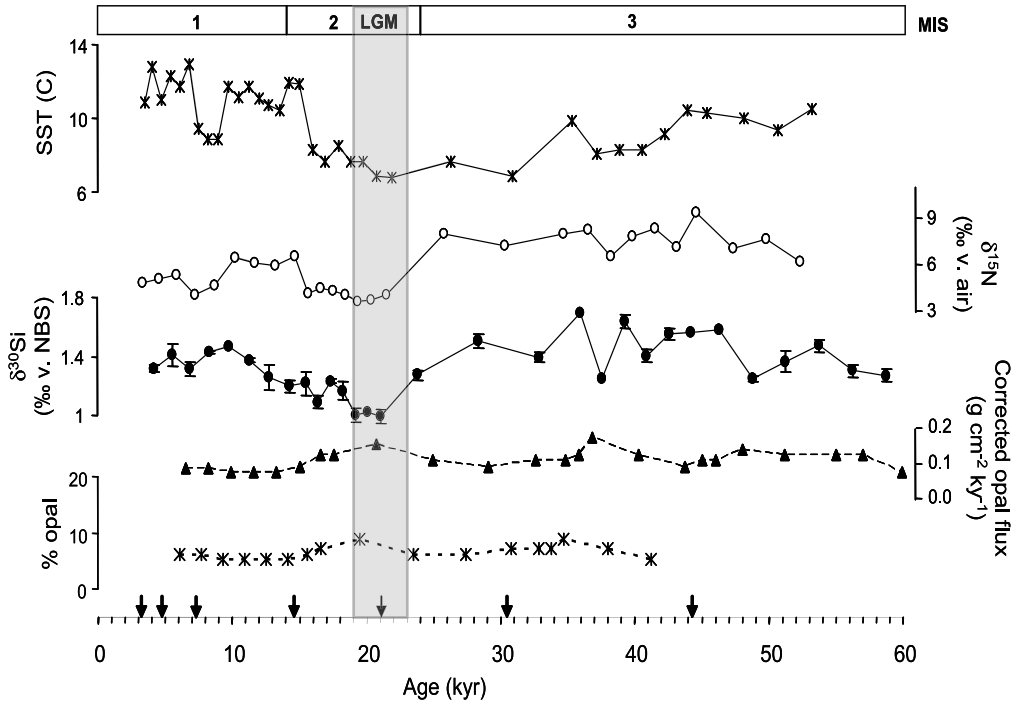

Figure 3. Down-core profiles of estimated sea surface temperature (SST), diatom-bound nitrogen isotopes, δ^{15}N [*Crosta et al.*, 2005], and diatom-silicon isotopes, δ^{30}Si, versus age from subtropical core MD97-2101. Error bars on δ^{30}Si represent 1 standard deviation. Black arrows represent the location of the ^{14}C ages. Opal content (% opal) and Th-normalized and dissolution-corrected opal rain rates are derived from nearby core MD94-102 [*Dézileau et al.*, 2000, 2003].

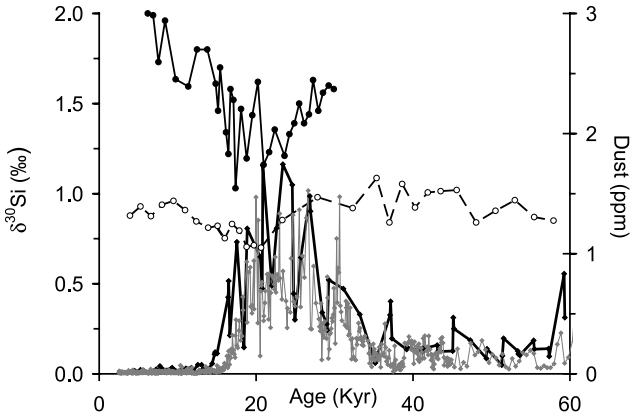

Figure 4. Comparison of Vostok dust concentration (diamond, black line), EPICA Dome C dust concentration (diamond, grey line), and diatom silicon isotopes δ^{30}Si from subantarctic core MD88-769 (solid circles) and subtropical core MD97-2101 (open circles).

and silicon isotope records. This analysis shows that shifts in the silicon isotope record are always accompanied by a change in the opposite direction in the dust record (Figure 5b). These patterns are also supported by the EPICA Dome C dust record which shows a weak, but statistically significant, negative correlation with the δ^{30}Si record (R^2 = 0.22, n = 33, $p < 0.05$, data not shown). These correlations with dust records from the Antarctic continent support a role for Fe in driving changes in nutrient depletion patterns in the sub-Antarctic. However, our cores are located at a significant distance from Antarctica where changes in dust inputs may have been different from those over the continent. Computer models which provide estimates of dust inputs at the actual location of MD88-769 predict two- to ten-fold increases in the flux of dust to this site during the LGM [*Andersen et al.*, 1998; *Mahowald et al.*, 1999] providing additional support that Fe drove changes in silicic acid and nitrate use in the sub-Antarctic during the last glacial period.

3.2.2. Subtropics

[19] In the core from the subtropics the dust and δ^{30}Si records are also inversely correlated. δ^{30}Si values decline with the increase in dust during the first half of MIS 2 (20–24 kyr) and low values persist through the rest of MIS 2. The correlations with the dust record from Vostok and EPICA Dome C are weak, but they are statistically significant (R^2 = 0.24, n = 30, $p < 0.01$; Vostok; R^2 = 0.22, n = 30, p = 0.05, EPICA Dome C). These correlations do not appear to be driven by a physiological response of diatoms to increased dust inputs. Release from Fe stress should produce an inverse correlation between δ^{30}Si and diatom δ^{15}N which is not observed in MD97-2101 (Figure 3), but which is observed in the subantarctic record (Figure 2) and in records from the Antarctic [*Brzezinski et al.*, 2002]. The modern subtropical gyres are not high-nutrient low-chlorophyll regions experiencing Fe limitation and thus phytoplankton there would not be expected to respond to increased dust supply during glacial periods, although a significant reduction in dust could lead to Fe-limiting conditions. Models of dust inputs are equivocal regarding whether atmospheric dust sources were enhanced in this region of the subtropics during glacial periods. According to *Andersen et al.* [1998], MD97-2101 is located in an area which did not receive larger dust atmospheric deposition during the LGM, while the model of *Mahowald et al.* [1999] suggests deposition increased two- to five-fold. No models indicate a strong decrease in dust supply. The results of these models combined with the parallel nature of the N and Si isotopic records during the past 50,000 years suggest that any increase in Fe supply from dust during the last glacial period only added Fe to an already iron-replete system and did not significantly affect local silicic acid and nitrate dynamics in the subtropics.

3.3. Nutrient Sources

3.3.1. Sub-Antarctic

3.3.1.1. Holocene

[20] Comparison of our Si isotope record from the sub-Antarctic with previous records from the Antarctic reveals differences between these regions during the Holocene that are consistent with the circulation and nutrient dynamics in the modern Southern Ocean. The main sources of nutrients to the surface waters of the ACC are winter mixing and upwelling between the Southern ACC Front and the Polar Front driven by the westerly winds. These winds drive upwelled waters northward via Ekman drift to the sub-Antarctic where they become incorporated into SAMW [e.g., *Pollard et al.*, 2002; *Sarmiento et al.*, 2004]. The

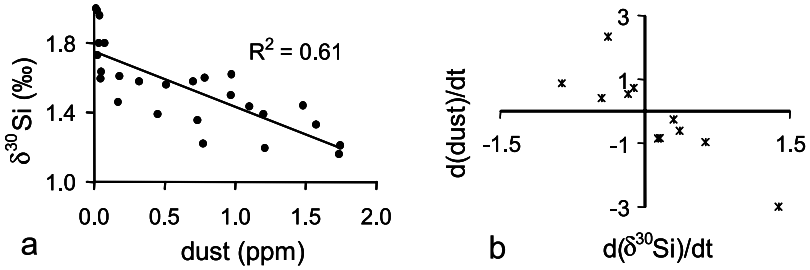

Figure 5. (a) The δ^{30}Si from subantarctic core MD88-769 versus Vostok dust concentration. (b) First derivative of silicon isotope δ^{30}Si from subantarctic core MD88-769 versus first derivative of dust from Vostok.

strong northward decline in the $Si(OH)_4$ concentrations in surface waters observed across the Antarctic is caused by the outcropping of shallower isopycnals to the north [*Pollard et al.*, 2002] and strong biological consumption of $Si(OH)_4$ [e.g., *Pondaven et al.*, 2000; *Sarmiento et al.*, 2004]. These trends combined with the fact that $\delta^{30}Si(OH)_4$ values decrease with depth in the near surface ocean and increase with $Si(OH)_4$ consumption by diatoms, results in an inverse relationship between the $\delta^{30}Si(OH)_4$ and its concentration across the ACC [*Varela et al.*, 2004; *Cardinal et al.*, 2005].

[21] The measured $\delta^{30}Si$ values in the subantarctic core MD88-769 averaged +1.9‰ (Table 1) (range +1.64 to +2.00‰) during the Holocene. That average is more positive than the value of ~1.3‰ predicted by the oceanic silicon isotope distribution model of *Wischmeyer et al.* [2003], but it agrees with direct measures of the $\delta^{30}Si$ of diatoms in surface waters of the modern Subantarctic Ocean [*Varela et al.*, 2004; *Cardinal et al.*, 2005]. It is more positive than Holocene $\delta^{30}Si$ values from the Indian Antarctic zone (range +1.2 to +1.5‰, average +1.4‰; Table 1 [*De La Rocha et al.*, 1998]). This change in $\delta^{30}Si$ between zones is consistent with the circulation and nutrient consumption patterns described above. Diatom growth in the Antarctic increases the $\delta^{30}Si(OH)_4$ in surface waters relative to that in the deep waters upwelling in the Antarctic. As Ekman drift transports these waters into the sub-Antarctic, additional diatom growth further increases the $\delta^{30}Si(OH)_4$ of the surface pool of $Si(OH)_4$ and the $\delta^{30}Si$ of diatoms growing on this pool increases consequently.

[22] In contrast to the $\delta^{30}Si$, diatom-bound $\delta^{15}N$ shows little to no change between the Indian sub-Antarctic and the Indian Antarctic during the Holocene averaging ~3‰ in the Antarctic [*Robinson et al.*, 2004] and 3‰ [*Crosta et al.*, 2005] to 4.5‰ [*Robinson et al.*, 2005] in the sub-Antarctic. The fact that the $\delta^{15}N$ does not show a clear increase between Antarctic and the sub-Antarctic appears inconsistent with an Antarctic source of nutrients to the sub-Antarctic. However, the uniformity of $\delta^{15}N$ may be related to changes in the magnitude of fractionation factor, ε, for nitrate assimilation between the sub-Antarctic and the Antarctic. Indeed, *DiFiore et al.* [2006] suggest that ε changes from ~+8‰ in the sub-Antarctic to +5‰ in the Antarctic. The $\delta^{15}N$ of the phytoplankton equals the $\delta^{15}NO_3^-$ of the source nitrate minus the isotope factor ε. Therefore the higher fractionation in the sub-Antarctic could compensate the higher $\delta^{15}NO_3^-$ of the nitrate delivered to the sub-Antarctic from the Antarctic zone minimizing the difference in $\delta^{15}N$ between the Antarctic and subantarctic diatoms.

3.3.1.2. LGM

[23] Variations in the silicon isotope record from the sub-Antarctic parallel those from previous records from the Antarctic [*De La Rocha et al.*, 1998]. Both records display a minimum in $\delta^{30}Si$ at the LGM; however, $\delta^{30}Si$ values in the sub-Antarctic are 0.5‰ more positive than those found in the Antarctic both during the LGM and during the Holocene (Table 1). Assuming that Antarctic waters were a major source of nutrients to the sub-Antarctic during both the LGM and the Holocene, then the nearly constant offset (0.5‰) in $\delta^{30}Si$ between the two regions suggests that phytoplankton growth in the sub-Antarctic consumed a similar percentage of the $Si(OH)_4$ entering from the Antarctic during both periods. However, opal rain rates in the sub-Antarctic were nearly three times higher during the LGM (0.26 g cm^{-2} kyr^{-1}) compared to the Holocene (0.10 g cm^{-2} kyr^{-1}, Figure 2). The only way to support greater rain rates while utilizing a similar percentage of the surface $Si(OH)_4$ pool is for that pool to increase in size. Thus the comparison of the isotopic records with the record of opal rain rates suggests that the pool of unused $Si(OH)_4$ in subantarctic surface waters was larger in absolute terms during glacial times compared to the Holocene. This is the first evidence from silicon isotopes that the increase in the size of the pool of unused $Si(OH)_4$ previously inferred for the glacial Antarctic [*Brzezinski et al.*, 2002] also occurred in the glacial sub-Antarctic. Thus, if the supply of $Si(OH)_4$ from the Antarctic to the sub-Antarctic during the LGM was similar to that occurring during the Holocene, then biological processes in the sub-Antarctic maintained an excess of $Si(OH)_4$ in subantarctic surface waters as required by the SALH.

3.3.2. Subtropics

3.3.2.1. Holocene

[24] The sub-Antarctic does not appear to be the major source of $Si(OH)_4$ to the subtropics in the vicinity of MD97-2101 during the Holocene. $\delta^{30}Si$ values in the subantarctic and the subtropical cores diverge strongly during the Holocene with lower values in the subtropics (~+1.4‰) compared to those in the sub-Antarctic (~+1.9‰) (Table 1). If diatoms in the subtropics were consuming nutrients coming from the sub-Antarctic the $\delta^{30}Si$ values from MD97-2101 should at least be equal to, if not higher than, those from comparable age strata in MD88-769. The fact that the $\delta^{30}Si$ values in the subtropics are consistently lower than the corresponding values from the sub-Antarctic argues that the sub-Antarctic was not the source of $Si(OH)_4$ to the subtropics during the Holocene. An alternative source could have been water coming from the subtropical gyre, but those nutrient-depleted oligotrophic waters would have had relative high $\delta^{30}Si(OH)_4$ (~+2.5‰) based on the model of *Wischmeyer et al.* [2003] and empirical observations in an oligotrophic gyre [*Reynolds et al.*, 2006]. Another source that could explain the low $\delta^{30}Si$ values observed in MD97-2101 is the retroflection of the Agulhas current. Many studies [e.g., *Belkin and Gordon*, 1996; *Sparrow et al.*, 1996] show that the retroflection and associated Agulhas Front (AF) can be traced up to 80°E at latitudes between 40°S and 45°S. According to the silicon isotope distribution model of *Wischmeyer et al.* [2003], the $\delta^{30}Si(OH)_4$ values in the Agulhas current region (southeast Africa) are low (<+1‰) and less positive than the ones in the subantarctic or the subtropical regions.

3.3.2.2. LGM

[25] The role of the sub-Antarctic as a source of dissolved Si to the subtropics during the LGM is unclear. The $\delta^{30}Si$ in the subtropics is lower than in the sub-Antarctic during the LGM (difference = 0.3‰), but the difference is less than observed during the Holocene (difference = 0.5‰). The opal rain rate in the subtropics is higher during the LGM

compared to the Holocene (0.16 versus 0.09 g cm^{-2} yr^{-1}, Figure 3) suggesting that opal production in surface waters increased in the subtropics during the LGM. Again, if the sub-Antarctic was the sole source of $Si(OH)_4$ to the subtropics then the $\delta^{30}Si$ of diatoms from the subtropics should have been more positive than that from the sub-Antarctic, which was not observed. These observations can be reconciled if the source of dissolved silicon to the subtropics was a combination of subantarctic waters with high $\delta^{30}Si(OH)_4$ combined with waters from the oligotrophic gyre and from the Agulhas Front with low $\delta^{30}Si(OH)_4$. The smaller difference in $\delta^{30}Si$ between the subtropics and the sub-Antarctic during the LGM compared to the Holocene could imply a larger role for the sub-Antarctic (the source with high $\delta^{30}Si(OH)_4$ as opposed to the Agulhas source with low $\delta^{30}Si(OH)_4$) in supplying dissolved Si to the subtropics during the LGM. While a stronger subantarctic influence during the LGM is consistent with increases in northward Ekman transport due to stronger zonal winds during glacial periods [e.g., *Rintoul and England*, 2002] this hypothesis is highly speculative.

3.4. Estimating the Silicic Acid Leakage From $\delta^{30}Si$ Records

[26] We constructed a simple isotope mass balance model to estimate the silicic acid content of SAMW during the Holocene and during the LGM. We first estimate the level of $Si(OH)_4$ use in the Antarctic to determine the size and isotopic composition of the pool of unused $Si(OH)_4$ in that zone. We assume that this unused $Si(OH)_4$ is transported to the sub-Antarctic and then we use its estimated isotopic composition and the measured isotopic value of the opal deposited in the sub-Antarctic to constrain the extent of silicic acid consumption in the subantarctic zone. The $Si(OH)_4$ remaining in subantarctic surface waters after opal production is assumed to be incorporated into SAMW. Since the results are highly sensitive to the choice of an open or closed isotope model we apply both.

[27] In this simple model, we assume a constant upwelling and a constant mixed layer depth which results in a constant Ekman flux across the Antarctic and sub-Antarctic. Therefore the flux of water upwelling in the Antarctic equals the flux of water flowing from the Antarctic surface waters to the subantarctic surface waters and the flux of water leaving the sub-Antarctic during mode water formation. The nutrient content of the upwelled water is influenced by biological production. With the assumption of a constant flux of water changes in silicic acid and biogenic silica concentrations between compartments are proportional to their fluxes. The model results are presented in terms of silicic acid concentration changes to facilitate the comparison with known data. In what follows we first assume equal fluxes of upwelled water between the Holocene and Last Glacial Maximum and then (section 3.5) explore the effect of possible increased stratification during the glacial period by reducing the upwelling flux during the ice age by an order of magnitude.

3.4.1. Si Dynamics in the Antarctic

[28] In the Antarctic, we first make the assumption that the system is open with a continuous supply of nutrients. This is appropriate for the Holocene because nutrients were supplied by persistent wind-driven upwelling [e.g., *Anderson et al.*, 2002]. The strength and consistency of upwelling during the LGM is unresolved; some studies suggest similar or more intense upwelling during the LGM than during the Holocene [e.g., *Keeling and Visbeck*, 2001] and others suggest reduced upwelling [e.g., *François et al.*, 1997; *Toggweiler et al.*, 2006]. Initially, we consider upwelling to have been similar during the two periods and then we assess the effects of a possible reduced upwelling during the LGM in section 3.5.

[29] The open system model for the Antarctic during both the Holocene and the LGM uses the equations outlined by *Varela et al.* [2004] describing the change in the isotopic composition of biogenic silica $\delta^{30}Si_{bSiO2}$ as a function of $Si(OH)_4$ use with a continuous supply of silicic acid,

$$\delta^{30}Si_{bSiO2} = \delta^{30}Si(OH)_{4init.} + \varepsilon \times f, \quad (1)$$

where f is the fraction of $Si(OH)_4$ remaining in the water after consumption, ε is the fractionation factor (−1.1‰), and $\delta^{30}Si(OH)_{4init.}$ is the $\delta^{30}Si(OH)_4$ value in the deep water upwelled to the surface. We use the measured values of $\delta^{30}Si$ in opal ($\delta^{30}Si_{bSiO2}$) and an estimate of $\delta^{30}Si(OH)_{4init.}$ to calculate the fraction of the $Si(OH)_4$ source (f) remaining in Antarctic surface waters after diatom growth both during the Holocene and during the LGM.

[30] The value of $\delta^{30}Si_{bSiO2}$ in the Antarctic is taken to be the $\delta^{30}Si$ of opal in core E50-11 (55°56′S–104°57′E, water depth 3923 m [*De la Rocha et al.*, 1998]), which is the closest core from the Indian Antarctic sector to the location of MD88-769 with a $\delta^{30}Si$ record. $\delta^{30}Si$ averages +1.4‰ for the Holocene and +0.9‰ for the LGM in E50-11 (Table 1; the other available core in the Indian sector RC11-94 has comparable average $\delta^{30}Si$ for the Holocene and the LGM [*De La Rocha et al.*, 1998]). There are no data on the silicon isotopic composition of $Si(OH)_4$ from near the locations of our cores to use in estimating $\delta^{30}Si(OH)_{4init.}$ We use the value of +1.7‰ measured at the depth of the winter mixed layer (~300 m [*Kara et al.*, 2003]) in the eastern part of the Indian Sector of the Antarctic Zone [*Cardinal et al.*, 2005] at the latitude of Antarctic core E50-11 (56°S) as our estimate of $\delta^{30}Si(OH)_{4init.}$ In making this estimate we multiplied the $\delta^{29}Si$ reported by *Cardinal et al.* [2005] of +0.85‰ by 1.96 to obtain the corresponding value of $\delta^{30}Si$ [*Brzezinski et al.*, 2006]. Then, using a value of −1.1‰ for the fractionation factor, ε [*De La Rocha et al.*, 1997], we estimate from equation (1) that 27% of the $Si(OH)_4$ supply remains in the surface waters of the Antarctic after diatom growth (f = 0.27) during the Holocene and that 73% remains during the LGM (f = 0.73) (Figure 6).

[31] Considering that waters upwelling in the Antarctic have an average silicic acid concentration of 65 μM (US JGOFS Southern Ocean website), we partition this $Si(OH)_4$ supply between diatom opal and unused $Si(OH)_4$ on the basis of the calculated values of f. Thus during the Holocene, 47 μM are used to produce opal and 18 μM are left behind in the Antarctic surface waters. This pattern reversed during the LGM with 18 μM used to produce opal and with 47 μM remaining as $Si(OH)_4$ in Antarctic surface waters.

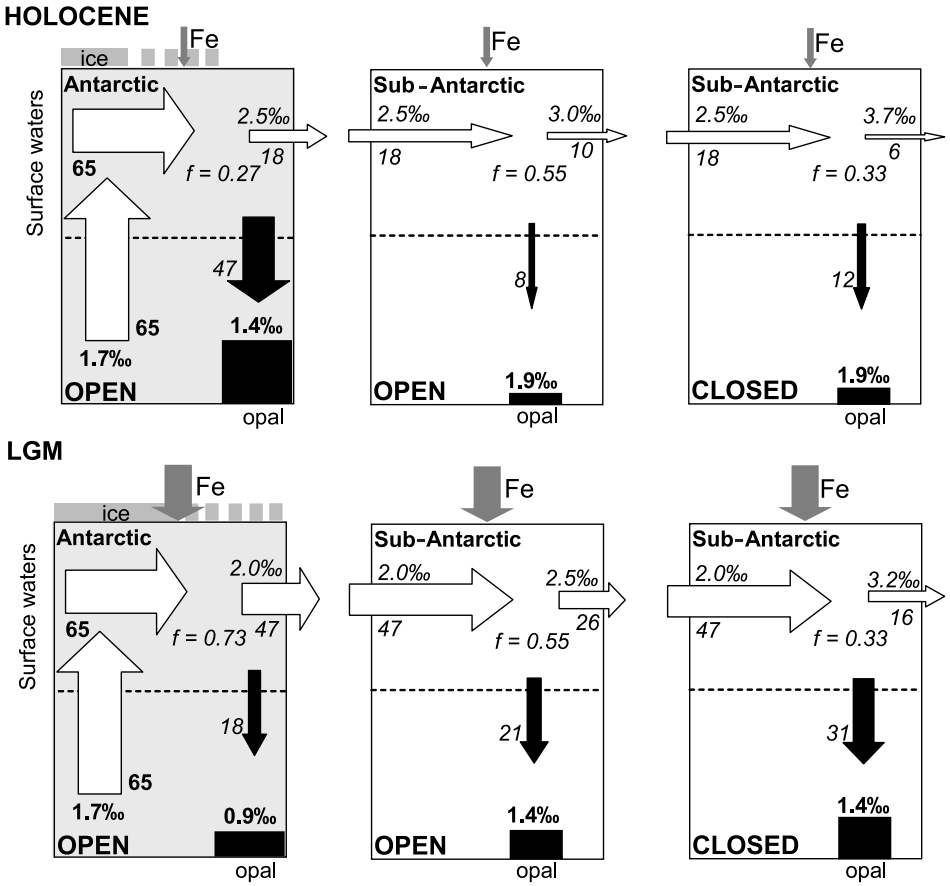

Figure 6. Schematic Si dynamic (in micromoles per liter) in the Antarctic and the subantarctic zones of the Indian Southern Ocean during the Holocene and the LGM. Data in bold are extracted from the literature and from this study (see text), and data in italics are calculated using a simple isotope mass balance model. White arrows represent silicic acid, black arrows represent biogenic silica, f is the fraction of silicic acid remaining in the water, and open and closed refer to the open and closed system model for silicon isotope.

[32] We then calculate the $\delta^{30}Si(OH)_4$ of the residual $Si(OH)_4$ in the surface waters of the Antarctic using the following open system model equation [*Varela et al.*, 2004]:

$$\delta^{30}Si(OH)_4 = \delta^{30}Si(OH)_{4init} - \varepsilon \times (1 - f). \quad (2)$$

The resulting values of $\delta^{30}Si(OH)_4$ are +2.5‰ and +2.0‰ for the Holocene and the LGM, respectively (Figure 6).

3.4.2. Si Dynamics in the Sub-Antarctic

[33] In the sub-Antarctic we assume that the only source of $Si(OH)_4$ to this region is the northward transport of Antarctic surface waters (this assumption will be relaxed later). Therefore the source of $Si(OH)_4$ to the sub-Antarctic has the characteristics calculated above for the residual silicic acid in Antarctic surface waters. The source is thus 18 μM with $\delta^{30}Si(OH)_4$ = +2.5‰ in the Holocene and 47 μM with $\delta^{30}Si(OH)_4$ = +2.0‰ during the LGM. Present knowledge of circulation in the sub-Antarctic does not allow us to choose between the open and the closed isotope models, so we present the results obtained using both models.

[34] We use the same procedure as described above for the Antarctic to predict the fraction of the supply of $Si(OH)_4$ that remains in subantarctic surface waters after producing opal with our measured $\delta^{30}Si$ of +1.9‰ during the Holocene and +1.4‰ during the LGM (Table 1). This calculation is performed using both the open and closed system isotope models (Figure 6). The equations for the open isotope model were given above. Those for a closed system are

$$\delta^{30}Si_{bSiO2} = \delta^{30}Si(OH)_{4init.} - \varepsilon \times (f \ln(f)/1 - f) \quad (3)$$

$$\delta^{30}Si(OH)_4 = \delta^{30}Si(OH)_{4init.} + \varepsilon \times \ln(f). \quad (4)$$

[35] We calculate that between 55% (open system estimate) and 33% (closed system estimate) of the $Si(OH)_4$ supply remains in subantarctic surface waters during both the Holocene and during the LGM (Figure 6). During the Holocene we calculate that between 6 and 10 μM $Si(OH)_4$

remains in subantarctic surface waters to be incorporated into SAMW. During the LGM, that amount almost triples to between 16 μM and 26 μM (Figure 6). The residual $Si(OH)_4$ has a calculated $\delta^{30}Si(OH)_4$ of between +3.0‰ and +3.7‰ (open and closed models, respectively) during the Holocene and between +2.5‰ and +3.2‰ (open and closed models, respectively) during the LGM (Figure 6). Values of $\delta^{30}Si(OH)_4$ in highly depleted surface waters have been measured to be between +2.5 and +3.2‰ [*Cardinal et al.*, 2005; *Reynolds et al.*, 2006; C. P. Beucher et al., unpublished data, 2006]. Values as high as the +3.7‰ predicted by the closed system model have not been observed in the modern ocean suggesting that the results from the open system model may better reflect nutrient dynamics in the sub-Antarctic.

[36] When we repeat this entire exercise using closed system model for the Antarctic we obtain impossible results. For the Holocene, the calculated $\delta^{30}Si(OH)_4$ of the silicic acid source in the sub-Antarctic is such that the observed isotopic signature of the sedimentary opal (+1.9‰) cannot be produced given known fractionation ($\varepsilon = -1.1$‰). For the LGM, almost no opal is deposited in the sub-Antarctic which runs counter to the increase of opal accumulation rates observed in this zone during the last glaciation [e.g., *François et al.*, 1997; *Chase et al.*, 2003; *Dézileau et al.*, 2003] and the known northward shift in the opal belt beneath the ACC during glacial times. We thus reject the closed system model for the Antarctic.

[37] The results of our isotope mass balance calculations shown in Figure 6 reproduce many observed features of opal deposition in the Southern Ocean during the Holocene with higher levels of opal accumulation in the Antarctic compared to the sub-Antarctic [e.g., *De Master*, 2002]. During the LGM, the results are consistent with measured declines in opal accumulation in the Antarctic and with observed increases in opal accumulation in the sub-Antarctic [*Chase et al.*, 2003; *Dézileau et al.*, 2003]. The predicted northward shift in the region of maximum opal deposition during the LGM is consistent with the combined effect of decreased silicic acid uptake under iron-enrichment coupled with any decrease in diatom production in the Antarctic sector caused by increased sea ice cover during the ice age [*Anderson et al.*, 2002; *Kohfeld et al.*, 2005]. The calculated ratio of opal deposition during the LGM to that during the Holocene in the sub-Antarctic is ~2.6 which is consistent with the ratio of 2.6 measured by *Dézileau et al.* [2003] for MD88-769. The sum of the $\delta^{30}Si(OH)_4$ used to produce the opal deposits beneath the Antarctic and subantarctic zones of the Indian Southern ocean is predicted to be lower during the LGM (39 to 49 μM) than during the Holocene (55 to 59 μM) in agreement with the observed decline in total opal accumulation (Antarctic + sub-Antarctic) in this region during the LGM [*Dézileau et al.*, 2003].

[38] The budget presented in Figure 6 can be used to predict patterns of nitrate use in the Indian Southern Ocean assuming that diatoms are the main consumers of nitrate. The literature gives an estimate of 35 μM for the concentration of nitrate in upwelled water in the present-day Antarctic [e.g., *Sigman and Boyle*, 2000]. Using a Si:N uptake ratio of ~4 during the Holocene [*Pondaven et al.*, 2000, and references therein], our estimated $Si(OH)_4$ depletion of 47 μM would have depleted 12 μM NO_3^- (47/4) in the Antarctic, i.e., a third of the source. Another 2 to 3 μM of nitrate would have been consumed in the sub-Antarctic leaving 20 μM to have been incorporated into SAMW during the Holocene consistent with observed values in the modern Southern Ocean [*Sarmiento et al.*, 2004].

[39] To estimate nitrate use during the LGM lower values of diatom Si:N uptake ratios are required to simulate the effect of enhanced Fe supply on diatom nutrient physiology. The appropriate uptake ratio likely lies somewhere between the value of 1:1 observed for nutrient-replete temperate diatoms [*Brzezinski*, 1985] and the value of 1:1 to 2:1 observed during iron enrichment experiments in the Southern Ocean [*Boyd et al.*, 2001; *Coale et al.*, 2004; *Franck et al.*, 2003]. At a Si:N depletion ratio of 1 nitrate depletion would have been 18 μM in the Antarctic during the LGM, which represents half of the source. The other half would have been entirely consumed in the sub-Antarctic. At a $[Si(OH)_4]:[NO_3^-]$ depletion ratio of 2:1 nitrate use in the glacial Antarctic would have been 9 μM with and additional 11 to 16 μM having been consumed in the sub-Antarctic leaving 10 to 15 μM to have been incorporated into SAMW. Thus we can only constrain the nitrate content of SAMW during the LGM to be between 0 and 15 μM. This represents a greater degree of nitrate depletion in the sub-Antarctic during the LGM compared to the Holocene in agreement with the results of *Robinson et al.* [2005]. However, refining these estimates is vital to test the SALH because an increased Si leakage to lower latitudes without a concomitant source of N would result in N limitation and little diatom growth at low latitudes.

3.5. Effects of Highly Stratified Antarctic Waters

[40] In this section we explore the effects of stratification in the Antarctic on Si leakage. Several studies invoke an increase in stratification of the Antarctic waters during the LGM to reconcile low opal accumulation rates with high values of $\delta^{15}N$ in sedimentary organic matter [e.g., *François et al.*, 1997; *Frank et al.*, 2000; *Sigman and Boyle*, 2000; *Toggweiler et al.*, 2006]. Enhanced stratification could have been caused by an equatorward shift of the westerly winds that drive the upwelling and/or a change in salinity implied by extended ice coverage [e.g., *Sigman and Boyle*, 2000]. *François et al. 1997*] invoke an order of magnitude reduction in the rate of upwelling in the glacial Antarctic to explain their $\delta^{15}N$ data. Figure 7 illustrates the effects of a tenfold decrease in the amount of upwelled water on our silicon isotope mass balance calculations. We simulated that decrease by reducing the concentration of $Si(OH)_4$ in surface waters from 65 μM to 7 μM and apply the previous f estimates of 0.73 in the Antarctic and 0.55 in the sub-Antarctic to calculate $Si(OH)_4$ consumption in the Antarctic and sub-Antarctic during the LGM (Figure 7). Those calculations indicate that opal production consumes 2 μM in the Antarctic with another 2 and 3 μM consumed in the sub-Antarctic for the open and closed models, respectively. Those values are much lower than calculated for either the Antarctic or sub-Antarctic during the Holocene (Figure 6). Thus, with a highly stratified Antarctic our model yields

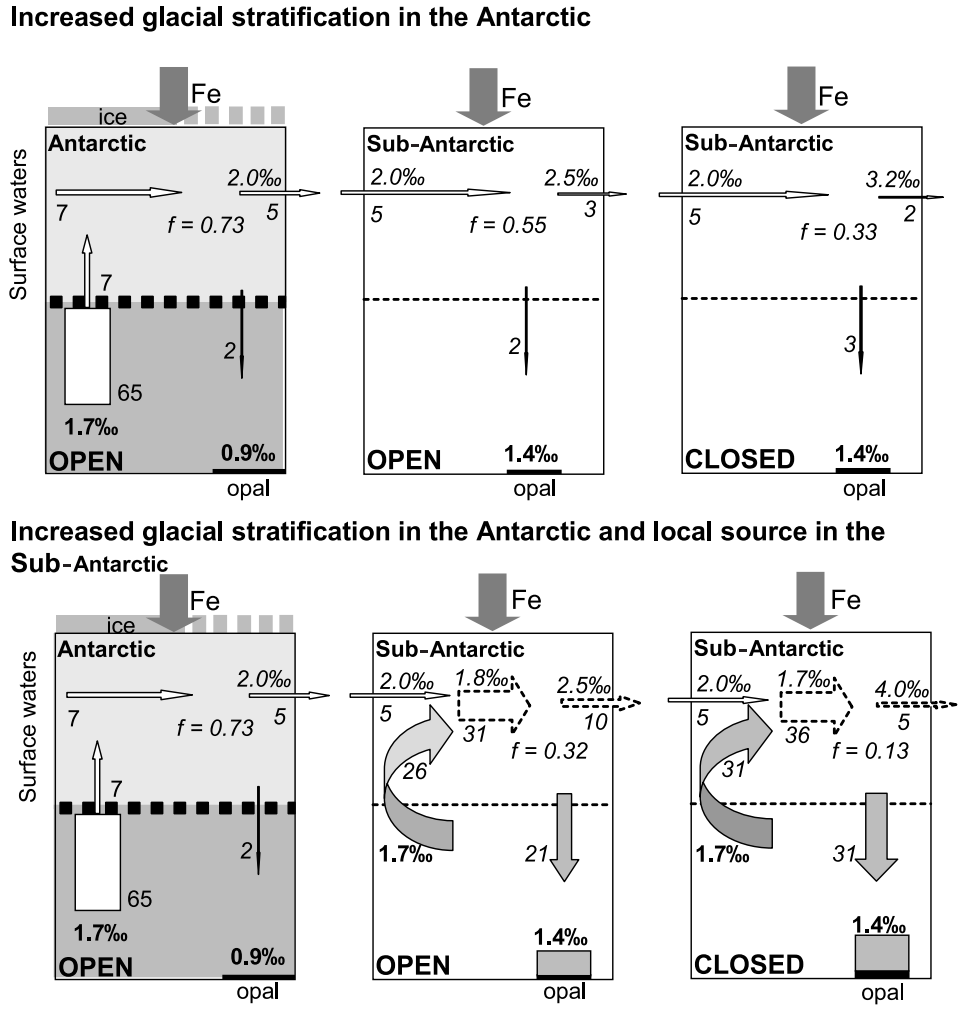

Figure 7. Schematic Si dynamic (in micromoles per liter) in the Antarctic and the subantarctic zones of the Indian Southern Ocean during the LGM in the increased stratification hypothesis. The curved arrow in the sub-Antarctic represents $Si(OH)_4$ supplied by a hypothetical enhancement of vertical mixing in this zone during the LGM. Opal from this source is indicated by the stripes on the bar representing opal

results that are at odds with the observed increase in opal accumulation in the sub-Antarctic during the LGM [*Dézileau et al.*, 2003; *Chase et al.*, 2003].

[41] In order to reconcile the low opal fluxes predicted by the model with the δ^{30}Si data while maintaining the assumption of a highly stratified Antarctic Ocean, we must invoke a large local source of $Si(OH)_4$ in the sub-Antarctic during glacial times (Figure 7). Such a source may be driven by a northward shift in the westerly winds during the last glacial period that would drive upwelling within the sub-Antarctic during cold periods [e.g., *Sigman and Boyle*, 2000]. On the basis of the data of *Cardinal et al.* [2005], the $Si(OH)_4$ in the sub-Antarctic at the depth of winter mixing (we assume that upwelling brings waters from no deeper than 300 m [*Kara et al.*, 2003]) has about the same $\delta^{30}Si(OH)_4$ values as the waters upwelling in the Antarctic, i.e., +1.7‰. We use this value in the isotope mass balance calculation to determine the increase in $Si(OH)_4$ concentration due to a local source in the sub-Antarctic which when combined to the small input of $Si(OH)_4$ from the sub-Antarctic produces opal sediments in the sub-Antarctic of the same magnitude and isotopic composition given by the nonstratified model (i.e., 21 μM and 31 μM $Si(OH)_4$ converted to opal in the open and closed models, respectively, with the opal having the observed δ^{30}Si of +1.4‰ in each case). We find that the local source has to raise surface $[Si(OH)_4]$ by 26 μM in the open model, and 31 μM with the closed model (Figure 7).

[42] Including the local source in the sub-Antarctic increases Si leakage from 2 to 3 μM to 5 to 10 μM (Figure 7) which is nearly identical to that estimated for the Holocene (Figure 6). In other words, with highly stratified Antarctic waters there would be no increased leakage of silicic acid to the lower latitudes during the LGM. However, this hypothesis requires a source of $Si(OH)_4$ that raises surface water in concentration by 26 to 31 μM in the sub-Antarctic

in order to produce the same opal deposition during the LGM as occurs in our model without stratification. Such high $Si(OH)_4$ concentrations are found at depths >500 m in the modern Indian sub-Antarctic well below the 300 m depth range currently involved in winter convective mixing (WOCE Hydrographic Atlas, BOT-I8, World Ocean Circulation Experiment, http://woce.nodc.noaa.gov/wdiu/). This, reconciling the stratified Antarctic scenario with known patterns of opal deposition and our Si isotope records requires significant changes to the subsurface nutrient field and circulation patterns within the sub-Antarctic during the LGM. A northward shift in the westerly winds around Antarctica may have intensified upwelling in the glacial sub-Antarctic [*Sigman and Boyle*, 2000], but several data sets place these winds at or to the south of their current position over the Antarctic during the LGM where they would not have enhanced upwelling in the sub-Antarctic (reviewed by *Anderson et al.* [2002]). Without a mechanism to produce a large local source of silicic acid in the glacial sub-Antarctic the silicon isotope records cannot be reconciled with enhanced stratification in the glacial Antarctic.

4. Conclusion

[43] Our silicon isotopic records imply less silicic acid depletion in the subantarctic zone during the LGM in the Indian sector of the Southern Ocean as required by the SALH. Comparison of subantarctic $\delta^{30}Si$ and opal rain rate records suggests that the pool of unused $Si(OH)_4$ in the glacial sub-Antarctic was larger than during the Holocene. N and Si isotope records are inversely correlated in the sub-Antarctic implying a switch to lower relative silicic acid depletion, but greater relative nitrate depletion, in this zone during the LGM compared to the Holocene as documented previously for the Antarctic. The correlation between changes in the subantarctic $\delta^{30}Si$ record and the dust records from the Vostok ice core supports a major role for dust mediated changes in Fe supply in driving shifts in silicic acid and nitrate depletion in the glacial sub-Antarctic. Congruence between the nitrogen and silicon isotopic records from the subtropics implies that enhanced Fe supplies during the LGM had little impact on silicic acid and nitrate dynamics in that zone.

[44] Simple mass balance calculations show that the measured differences in $\delta^{30}Si$ between the Antarctic and sub-Antarctic are consistent with a significant increase in silicic acid leakage from the Southern Ocean during the LGM if upwelling and Ekman drift were similar to that occurring in the modern Southern Ocean. Stratification of the Antarctic during the LGM eliminates Si leakage in our simple model, but requires a strong local source of dissolved Si in the sub-Antarctic to reproduce the known increases in opal accumulation in this zone during glacial periods. The estimated magnitude of this source is inconsistent with present-day subsurface nutrient concentrations in this region requiring a significant rearrangement of Southern Ocean circulation and nutrient distributions to produce this effect. An improved understanding of how upper ocean circulation changed during glacial periods will be vital to future tests of the SALH.

[45] **Acknowledgments.** We would like to thank Janice Jones for assistance with the silicon isotope measurements and two anonymous reviewers for critical comments on the manuscript. This work was supported by OCE-0350576 from the National Science Foundation.

References

Altabet, M. A., and R. Francois (1994), Sedimentary nitrogen isotopic ratio as a recorder for surface ocean nitrate utilization, *Global Biogeochem. Cycles*, *8*, 103–116.

Andersen, K. K., A. Armengaud, and C. Genthon (1998), Atmospheric dust under glacial and interglacial conditions, *Geophys. Res. Lett.*, *25*(13), 2281–2284.

Anderson, R. F., Z. Chase, M. Q. Fleisher, and J. Sachs (2002), The Southern Ocean's biological pump during the Last Glacial Maximum, *Deep Sea Res., Part II*, *49*, 1909–1938.

Belkin, I. M., and A. L. Gordon (1996), Southern Ocean fronts from the Greenwich meridian to Tasmania, *J. Geophys. Res.*, *101*(C2), 3675–3696.

Boyd, P. W., A. C. Crossley, G. R. DiTullio, F. B. Griffiths, D. A. Hutchins, B. Quéquiner, P. N. Sedwick, and T. W. Trull (2001), Control of phytoplankton growth by iron supply and irradiance in the subantarctic Southern Ocean: Experimental results from the SAZ project, *J. Geophys. Res.*, *106*(C12), 31,573–31,584.

Brzezinski, M. A. (1985), The Si:C:N ratio of marine diatoms: Interspecific variability and the effect of some environmental variables, *J. Phycol.*, *21*, 347–357.

Brzezinski, M. A., D. M. Nelson, V. M. Franck, and D. E. Sigmon (2001), Silicon dynamics within an intense open-ocean diatom bloom in the Pacific sector of the Southern Ocean, *Deep Sea Res., Part II*, *48*, 3997–4018.

Brzezinski, M. A., C. J. Pride, V. Franck, D. M. Sigman, J. L. Sarmiento, K. Matsumoto, N. Gruber, G. H. Rau, and K. H. Coale (2002), A switch from $Si(OH)_4$ to NO_3^- depletion in the glacial Southern Ocean, *Geophys. Res. Lett.*, *29*(12), 1564, doi:10.1029/2001GL014349.

Brzezinski, M. A., J. L. Jones, C. P. Beucher, and M. S. Demarest (2006), Automated determination of silicon isotope natural abundance by the acid decomposition of cesium hexafluosilicate, *Anal. Chem.*, *78*(17), 6109–6114, doi:10.1021/ac0606406.

Cardinal, D., L. Y. Alleman, F. Dehairs, N. Savoye, T. W. Trull, and L. Andre (2005), Relevance of silicon isotopes to Si-nutrient utilization and Si-source assessment in Antarctic waters, *Global Biogeochem. Cycles*, *19*, GB2007, doi:10.1029/2004GB002364.

Charles, C. D., P. N. Froelich, M. A. Zibello, R. A. Mortlock, and J. J. Morley (1991), Biogenic opal in Southern Ocean sediments over the last 450,000 years: Implications for surface water chemistry and circulation, *Paleoceanography*, *6*(6), 697–728.

Chase, Z., R. F. Anderson, M. Q. Fleisher, and P. W. Kubik (2003), Accumulation of biogenic and lithogenic materials in the Pacific sector of the Southern Ocean during the past 40,000 years, *Deep Sea Res., Part II*, *50*, 799–832.

Coale, K. H., et al. (2004), Southern Ocean iron enrichment experiment: Carbon cycling in high- and low-Si waters, *Science*, *304*, 408–414.

Crosta, X., and A. Shemesh (2002), Reconciling down-core anti-correlation of diatom carbon and nitrogen isotopic ratios from the Southern Ocean, *Paleoceanography*, *17*(1), 1010, doi:10.1029/2000PA000565.

Crosta, X., A. Shemesh, J. Etourneau, R. Yam, I. Billy, and J. J. Pichon (2005), Nutrient cycling in the Indian sector of the Southern Ocean over the last 50,000 years, *Global Biogeochem. Cycles*, *19*, GB3007, doi:10.1029/2004GB002344.

De La Rocha, C. L., M. A. Brzezinski, and M. J. DeNiro (1996), Purification, recovery, and laser-driven fluorination of silicon from dissolved and particulate silica for the measurement of natural stable isotope abundances, *Anal. Chem.*, *68*, 3746–3750.

De La Rocha, C. L., M. A. Brzezinski, and M. J. DeNiro (1997), Fractionation of silicon isotopes during biogenic silica formation, *Geochim. Cosmochim. Acta*, *61*(23), 5051–5056.

De la Rocha, C. L., M. A. Brzezinski, M. J. DeNiro, and A. Shemesh (1998), Silicon-isotope composition of diatom as an indicator of past oceanic change, *Nature*, *395*, 680–683.

De Master, D. J. (2002), The accumulation and cycling of biogenic silica in the Southern Ocean: Revisiting the marine silica budget, *Deep Sea Res., Part II*, *49*, 3155–3167.

Dézileau, L., G. Bareille, J. L. Reyss, and F. Lemoine (2000), Evidence for strong sediment redistribution by bottom currents along the southeast Indian ridge, *Deep Sea Res., Part I*, *47*, 1899–1936.

Dézileau, L., J. L. Reyss, and F. Lemoine (2003), Late Quaternary changes in biogenic opal fluxes in the Southern Indian Ocean, *Mar. Geol.*, *202*, 143–158.

DiFiore, P. J., D. M. Sigman, T. W. Trull, M. J. Lourey, K. Karsh, G. Cane, and R. Ho (2006), Nitrogen isotope constraints on subantarctic biogeochemistry, *J. Geophys. Res.*, *111*, C08016, doi:10.1029/2005JC003216.

Elderfield, H., and R. E. M. Rickaby (2000), Oceanic Cd/P ratio and nutrient utilization in the glacial Southern Ocean, *Nature*, *405*, 305–310.

Franck, V. M., K. W. Bruland, D. A. Hutchins, and M. A. Brzezinski (2003), Iron and zinc effects on silicic acid and nitrate uptake kinetics in three high-nutrient, low-chlorophyll (HNLC) regions, *Mar. Ecol. Prog. Ser.*, *252*, 15–33.

Franck, V. M., G. J. Smith, D. A. Hutchins, and M. A. Brzezinski (2005), Comparison of size-dependent carbon, nitrate, and silicic acid uptake rates in high- and low-iron waters, *Limnol. Oceanogr.*, *50*(3), 825–838.

François, R., M. A. Altabet, E. F. Yu, D. M. Sigman, M. P. Bacon, M. Frank, G. Bohrmann, G. Bareille, and L. D. Labeyrie (1997), Contribution of Southern Ocean surface-water stratification to low atmospheric CO_2 concentrations during the last glacial period, *Nature*, *389*, 929–935.

Frank, M., R. Gersonde, M. R. van der Loeff, G. Bohrmann, C. Nurnberg, P. W. Kubik, M. Suter, and A. Mangini (2000), Similar glacial and interglacial export bioproductivity in the Atlantic sector of the Southern Ocean: Multiproxy evidence and implications for glacial atmospheric CO_2, *Paleoceanography*, *15*(6), 642–658.

Hutchins, D. A., and K. W. Bruland (1998), Iron-limited diatom growth and Si:N uptake ratios in a coastal upwelling regime, *Nature*, *393*, 561–564.

Kara, A. B., P. A. Rochford, and H. E. Hurlburt (2003), Mixed layer depth variability over the global ocean, *J. Geophys. Res.*, *108*(C3), 3079, doi:10.1029/2000JC000736.

Keeling, R. F., and M. Visbeck (2001), Antarctic stratification and glacial CO_2, *Nature*, *412*, 605–606.

Kohfeld, K. E., and S. P. Harrison (2001), DIRTMAP: The geological record of dust, *Earth Sci. Rev.*, *54*(1–3), 81–114.

Kohfeld, K. E., C. Le Quéré, S. P. Harrison, and R. F. Anderson (2005), Role of marine biology in glacial-interglacial CO_2 cycles, *Science*, *308*, 74–78.

Kumar, N., R. F. Anderson, R. A. Mortlock, P. N. Froelich, P. Kubik, B. Dittrich-Hannen, and M. Suter (1995), Increased biological productivity and export production in the glacial Southern Ocean, *Nature*, *378*, 675–680.

Mahowald, N., K. Kohfield, M. Hansson, Y. Balkanski, S. P. Harrison, I. C. Prentice, M. Schulz, and H. Rodhe (1999), Dust sources and deposition during the Last Glacial Maximum and current climate: A comparison of model results with paleodata from ice cores and marine sediments, *J. Geophys. Res.*, *104*(D13), 15,895–15,916.

Matsumoto, K., J. L. Sarmiento, and M. A. Brzezinski (2002), Silicic acid leakage from the Southern Ocean: A possible explanation for glacial atmospheric pCO_2, *Global Biogeochem. Cycles*, *16*(3), 1031, doi:10.1029/2001GB001442.

Mortlock, R. A., C. D. Charles, P. N. Froelich, M. A. Zibello, J. Saltzman, J. D. Hays, and L. H. Burkle (1991), Evidence for lower productivity in the Antarctic Ocean during the last glaciation, *Nature*, *351*, 220–223.

Nozaki, Y., and Y. Yamamoto (2001), Radium 228 based nitrate fluxes in the eastern Indian Ocean and the South China Sea and a silicon-induced "alkalinity pump" hypothesis, *Global Biogeochem. Cycles*, *15*, 555–567.

Pollard, R. T., M. I. Lucas, and J. F. Read (2002), Physical controls on biogeochemical zonation in the Southern Ocean, *Deep Sea Res., Part II*, *49*, 3289–3305.

Pondaven, P., D. Ruiz-Pino, C. Fravelo, P. Tréguer, and C. Jendel (2000), Interannual variability of Si and N cycles at the time-series station KERFIX between 1990 and 1995: A 1-D modeling study, *Deep Sea Res., Part II*, *47*, 223–257.

Reynolds, B. C., M. Frank, and A. N. Halliday (2006), Silicon isotope fractionation during nutrient utilization in the North Pacific, *Earth Planet. Sci. Lett.*, *244*(1–2), 431–443, doi:10.1016/j.epsl.2006.02.002.

Rintoul, S. R., and M. H. England (2002), Ekman transport dominates local air–sea fluxes in driving variability of subantarctic mode water, *J. Geophys. Oceanogr.*, *32*(5), 1308–1321, doi:10.1175/1520-0485.

Robinson, R. S., B. G. Brunelle, and D. M. Sigman (2004), Revisiting nutrient utilization in the glacial Antarctic: Evidence from a new method for diatom-bound N isotopic analysis, *Paleoceanography*, *19*, PA3001, doi:10.1029/2003PA000996.

Robinson, R. S., D. M. Sigman, P. J. DiFiore, M. M. Rohde, T. A. Mashiotta, and D. W. Lea (2005), Diatom-bound $^{15}N/^{14}N$: New support for enhanced nutrient consumption in the ice age sub-Antarctic, *Paleoceanography*, *20*, PA3003, doi:10.1029/2004PA001114.

Rosenthal, Y., E. A. Boyle, and L. Labeyrie (1997), Last Glacial Maximum paleochemistry and deepwater circulation in the Southern Ocean: Evidence from foraminiferal cadmium, *Paleoceanography*, *12*(6), 787–796.

Rosenthal, Y., M. Dahan, and A. Shemesh (2000), The glacial Southern Ocean: A source of atmospheric CO_2 as inferred from carbon isotopes in diatoms, *Paleoceanography*, *15*(1), 65–75.

Rosman, K. J. R., and P. D. P. Taylor (1998), Isotopic compositions of the elements: Technical report, *Pure Appl. Chem.*, *70*(1), 217–235.

Sarmiento, J. L., M. Gruber, M. A. Brzezinski, and J. P. Dunne (2004), High-latitude controls of thermocline nutrients and low latitude biological productivity, *Nature*, *427*, 56–60.

Sigman, D. M., and E. A. Boyle (2000), Glacial/interglacial variations in atmospheric carbon dioxide, *Nature*, *407*, 859–869.

Singer, A. J., and A. Shemesh (1995), Climatically linked carbon isotope variation during the past 430,000 years in Southern Ocean Sediments, *Paleoceanography*, *10*(2), 171–177.

Sparrow, M. D., K. J. Heywood, J. Brown, and D. P. Stevens (1996), Current structure of the south Indian Ocean, *J. Geophys. Res.*, *101*(C3), 6377–6392.

Takeda, S. (1998), Influence of iron availability on nutrient consumption ratio of diatoms in oceanic waters, *Nature*, *393*(6687), 774–777.

Toggweiler, J. R., J. L. Russell, and S. R. Carson (2006), Midlatitude westerlies, atmospheric CO_2, and climate change during the ice ages, *Paleoceanography*, *21*, PA2005, doi:10.1029/2005PA001154.

Varela, D. E., C. J. Pride, and M. A. Brzezinski (2004), Biological fractionation of silicon isotopes in Southern Ocean surface waters, *Global Biogeochem. Cycles*, *18*, GB1047, doi:10.1029/2003GB002140.

Wischmeyer, A. G., C. L. De La Rocha, E. Maier-Reimer, and D. A. Wolf-Gladrow (2003), Control mechanisms for the oceanic distribution of silicon isotopes, *Global Biogeochem. Cycles*, *17*(3), 1083, doi:10.1029/2002GB002022.

C. P. Beucher, Marine Science Institute, University of California, Santa Barbara, CA 93106, USA. (beucher@lifesci.ucsb.edu)

M. A. Brzezinski, Department of Ecology Evolution and Marine Biology and Marine Science Institute, University of California, Santa Barbara, CA 93106, USA. (brzezins@lifesci.ucsb.edu)

X. Crosta, UMR-CNRS 5805 EPOC, Université Bordeaux I, F-33405 Talence, France. (x.crosta@epoc.u-bordeaux1.fr)